Communications to the Editor

Shifting the Order−Disorder Transition Temperature of Block Copolymer Systems with Electric Fields

Heiko G. Schoberth,[†] Kristin Schmidt,[‡] Kerstin A. Schindler,[†] and Alexander Böker*,[§]

Lehrstuhl für Physikalische Chemie II, Universität Bayreuth, D-95440 Bayreuth, Germany; Materials Research Laboratory, University of California, Santa Barbara, California 93106; and Lehrstuhl für Makromolekulare Materialien und Oberflächen and DWI an der RWTH e.V., RWTH Aachen University, D-52056 Aachen, Germany

Introduction. For binary mixtures the phase separation depends on various typical parameters like pressure and temperature. In addition, in 1965 Debye and Kleboth showed that it can also be influenced by external electric fields. They found that a moderate electric field lowers the critical point of a mixture of low molecular weight components.[1] In 1993, Wirtz et al. proved the same for polymer solutions of homopolymers.[2] However, the behavior of block copolymer systems in melt and solution is still under debate as different theoretical approaches predict contrary effects of an electric field on different binary systems (polymer−solvent or polymer−polymer). On the one hand, the electric field favors mixing and reduces the order−disorder transition temperature (T_{ODT}).[3,4] On the other hand, composition fluctuations should be suppressed, weakening the phase transition, and therefore T_{ODT} shifts to higher temperatures under electric fields.[5] So far, theory only agrees that the observed effect should increase with increasing electric field strength.[2,6−10] However, in the past, it was anticipated that experimentally accessible electric fields would not be of sufficient strength to induce a measurable effect.[3]

Block copolymers self-assemble into various structures on length scales of 10−100 nm.[11] Because of the variety of possible applications, block copolymers are still a subject of interest, and aligning domains via an electric field is just one possible processing method leading to technically relevant structures.[12,13] Hence, a better understanding of the impact of electric fields on block copolymer systems is needed. In this Communication we present first experimental evidence for the electric field-induced decrease of the order−disorder transition temperature in a block copolymer. Because of the high melt viscosities, temperatures close to the decomposition temperature and extremely high electric field strengths are required to achieve a measurable effect. In recent studies, we have demonstrated that concentrated block copolymer solutions in a neutral solvent act like a melt, thereby effectively circumventing the above-mentioned limitations.[14−16]

Experimental Section. We synthesized a lamella forming polystyrene-*block*-polyisoprene diblock copolymer (SI) by sequential living anionic polymerization. SI consists of 46 wt % polystyrene and 54 wt % polyisoprene with a total number-average molecular weight $M_n = 108$ kg/mol and a polydispersity $M_w/M_n = 1.05$. The polymer was dissolved in toluene with a concentration of 32.5 wt %. The temperature-controlled experiments were performed in a home-built cubic capacitor designed for square (2 × 2 mm) glass tubes which fit in between the electrode spacing of 2 mm. The whole capacitor is filled with insulating oil which is also used to heat the sample. The oil temperature could be adjusted by an external temperature control system within ±0.05 K. The X-ray beam penetrates the sample in the center of the capacitor through two small tubes with diamond windows to reduce the background scattering from the oil. The whole setup will be described in detail elsewhere.

A dc voltage up to 20 kV was applied across the electrodes, resulting in a homogeneous electric field pointing perpendicular to the direction of the X-ray beam with a maximum strength of 10 kV/mm. Synchrotron SAXS measurements were performed at the ID2 beamline at the European Synchrotron Radiation Facility (ESRF, Grenoble, France). The diameter of the X-ray beam was 150 μm. The photon energy was set to 12.5 keV. SAXS patterns were recorded with a two-dimensional camera located at a distance of 5 m from the sample within an evacuated flight tube. An image intensified CCD detector was used, which can handle the full X-ray flux. The CCD detector is capable of acquiring continuously high-resolution images of 2048 × 2048

* Corresponding author. E-mail: boeker@dwi.rwth-aachen.de.
† Universität Bayreuth.
‡ University of California, Santa Barbara.
§ RWTH Aachen University.

pixels every 5 s. Prior to data analysis, background scattering was subtracted from the data, and corrections were made for spatial distortions and for the detector efficiency.

In order to determine T_{ODT}, the solution of SI was filled into the glass tube and sealed to avoid solvent evaporation. As the volume of the glass tube is small compared to the volume of the surrounding oil, the oil temperature in the capacitor cube was taken as the actual temperature of the sample. Next, we applied a constant heating rate of 1.25 °C/min starting below T_{ODT} with $T = 45$ °C. At $T = 62$ °C, above the order−disorder temperature, the temperature was kept constant for some minutes in order to equilibrate the system. Subsequently, the cooling cycle was started with a rate of −1.25 °C/min until $T = 45$ °C was reached. Again, we kept the temperature constant followed by the application of an electric field of $E = 3$ kV/mm. With the electric field we orient the lamellae parallel to the electric field vector as reported earlier.[17] After complete orientation, we applied a different electric-field strength and proceeded with the next heating and cooling cycle.[14,15] Note that we always oriented and equilibrated the sample at $E = 3$ kV/mm and $T = 45$ °C before each cycle to have the same starting conditions. To avoid systematic errors, we used a random sequence of electric-field strengths. In addition, we repeated the measurements for different electric-field strengths to ensure reproducibility.

To define general criteria for the order−disorder transition temperature, we used changes in the patterns of the 2D-SAXS images. The 2D scattering patterns show typical corrugated peaks for oriented lamellae as long as the system is in the phase separated regime (see Figure 1a). Heating the sample above T_{ODT} results in an isotropic intensity distribution. The azimuthal scattering reflects this behavior as can be seen in Figure 1b. For oriented lamellae parallel to the electric field vector the maximum intensity can be found at $\varphi = 0°$ and $\varphi = 180°$, whereas for an isotropic disordered state a uniform distribution is obtained. Therefore, we propose the orientational order parameter P_2 as a good indicator for the order−disorder transition. P_2 is calculated according to eqs 1 and 2 as previously described in ref 14:

$$P_2 = \frac{3\langle\cos^2\varphi\rangle - 1}{2} \qquad (1)$$

with

$$\langle\cos^2\varphi\rangle = \frac{\int_0^{2\pi} d\varphi(I_q(\varphi)\cos^2(\varphi)|\sin(\varphi)|)}{\int_0^{2\pi} d\varphi(I_q(\varphi)|\sin(\varphi)|)} \qquad (2)$$

Depending on the position of the maxima of the scattering intensity the order parameter P_2 ranges from −0.5 to 1, where negative values indicate the degree of orientation parallel to the electric field vector. An isotropic distribution of the scattering intensity results in an order parameter $P_2 = 0$.

As additional indicator for the order−disorder transition the characteristics of the one-dimensional scattering profile can be used.[18] Besides a narrow first-order peak, additional peaks of higher orders are visible below T_{ODT}. Above T_{ODT} all higher order peaks vanish, and a broad first-order peak remains which arises from the correlation hole scattering and does not change during further heating (see Figure 2).

Results and Discussion. During the heating and cooling cycles, we have continuously taken SAXS images every 5 s to document the evolution of the system. In Figure 1a we show four exemplary 2D SAXS patterns around the order−disorder transition during a heating cycle. The electric field strength was set to $E = 3$ kV/mm. Clearly a significant difference between the scattering patterns is observed. While heating the polymer solution the scattering becomes more and more isotropic; i.e., the degree of order decreases until a completely uniform intensity distribution is found. Figure 1b shows the corresponding azimuthal distribution of the scattering intensity. The time dependence of the order parameter P_2 and the corresponding temperature of the sample is shown in Figure 1c. Starting with $P_2 = -0.22$ the order parameter decreases during the heating cycle and reaches $P_2 \approx 0$ at $T = 53.3$ °C, which we determine as T_{ODT}^h (3 kV/mm) according to the conditions defined above. The points corresponding to the SAXS pattern in Figure 1a,b are marked in (c). P_2 remains constant until the temperature falls below T_{ODT}^c (3 kV/mm) during the cooling cycle. We can verify the order−disorder transition temperature by analyzing the 1D SAXS profile for the appearance of higher order peaks and the correlation hole scattering. Figure 2 presents a series of measurement starting at $T = 52.0$ °C. The higher order peaks vanish prior to the transition, while the azimuthal scattering distribution at $T = 53.0$ °C is still slightly anisotropic. Reaching $T = 53.3$ °C, the shape of the first-order peak does not change anymore, and also the azimuthal scattering intensity distribution becomes isotropic.

By performing the described analysis for every heating and cooling cycle for different electric field strengths in random order to exclude any possible effects of the sample history, we derived the dependence of T_{ODT} on the electric field strength, which is shown in Figure 3. We find a clear decrease of the T_{ODT} with increasing electric-field strength for the heating cycles. During the cooling the transition always occurs at the same temperature independent of the applied field. One would expect the same influence for both heating and cooling cycles. This discrepancy can be explained as follows: As we prealign the lamellae in the microphase-separated regime the system exhibits well-ordered and large domains. Therefore, the electric field can act on these domains and induce their melting during the heating process. In the case of the cooling of the system a kinetic effect comes into play. As long as the temperature is above $T_{ODT}^c = 53.8 \pm 0.2$ °C the system is disordered; i.e., there are no lamellar domains for the electric field to act on. As soon as the system starts to microphase separate, very small domains are generated which are too small to couple effectively to the electric field.[19] Since the cooling rate is too large, the temperature of the system is already below T_{ODT}^h before the electric field can act on the growing domains and suppresses the microphase separation. Hence, the system remains microphase separated. Therefore, this behavior depends strongly on the chosen cooling rate and follows T_{ODT}^h dependence only for very small cooling rates.

To verify this assumption, we changed the procedure in order to exclude kinetic effects. We heated the system 10 K over T_{ODT} without an electric field until it is completely disordered. In the disordered state we applied an the electric field of $E = 7$ kV/mm. Cooling very slowly down to $T = 53.0$ °C with a rate lower than −0.1 °C/min let the sample remain in the disordered state. The corresponding SAXS spectra are shown in Figure 4. Switching off the electric field at the same temperature results in microphase separation of the sample. The influence of the electric field could be considered as crossing the horizontal line of transition in the phase diagram. This transition is fully reversible since switching on and off the electric field toggles disordering and microphase separation of the sample. Further decreasing the temperature with an applied field of $E = 7$ kV/mm again induces microphase separation. This behavior confirms the general results that the electric field lowers the
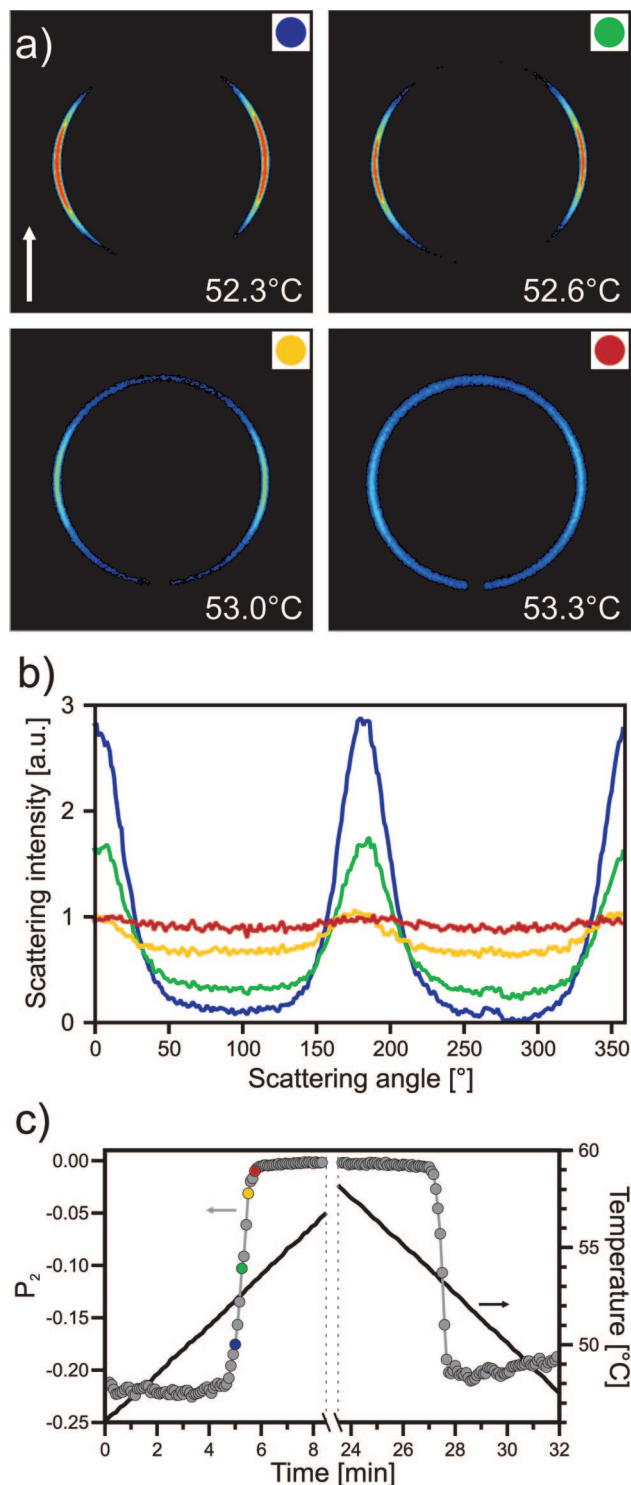
Figure 1. (a) 2D-SAXS images of a 32.5 wt % solution of SI in toluene under an electric field of 3 kV/mm at different temperatures as indicated. The arrow in the first image indicates the direction of the electric field vector. (b) Azimuthal scattering intensity after background subtraction and normalization. The curves corresponds to the sequence of images in (a). (c) Order parameter P_2 (●) and temperature (−) as a function of time. Colored points correspond to scattering patterns shown in (a) and (b).

order−disorder transition temperature as found during the heating cycle.

Conclusion. In conclusion, we have shown first experimental results for the influence of an electric field on the order−disorder transition temperature T_{ODT}. For fields as high as 8.5 kV/mm
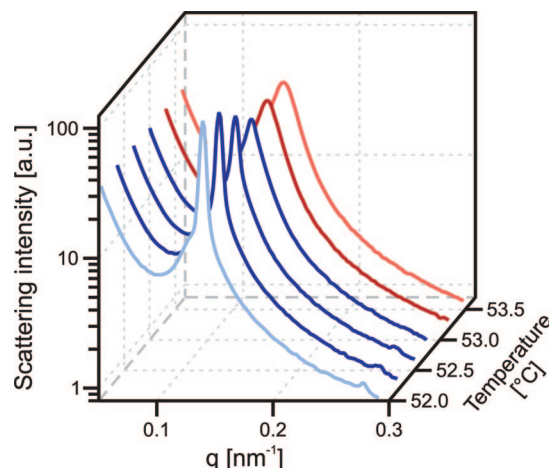

Figure 2. Time evolution of the SAXS spectra of a 32.5 wt % solution of SI in toluene exposed to an electric field of 3 kV/mm during heating cycle. The order−disorder temperature was determined to $T_{ODT} = 53.3$ °C. The red curves correspond to temperature above the T_{ODT} and the blue curves to temperatures below T_{ODT}. Data in dark colors correspond to the pattern shown in Figure 1.
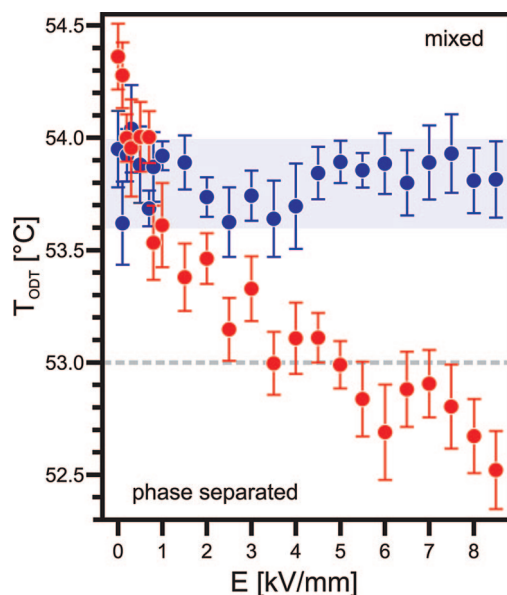

Figure 3. Order−disorder transition temperature T_{ODT} as a function of the electric-field strength E of a 32.5 wt % solution of SI in toluene. The temperatures have been obtained during cooling (blue ●) and heating cycles (red ●) of the solution. The gray dashed line at $T = 53.0$ °C refers to the constant temperature experiment in Figure 4.

we find a decrease in the T_{ODT} by more than 1.5 K. Furthermore, we found that the cooling rate has a strong impact on the order−disorder transition temperature during cooling. For a high cooling rate the disorder−order transition occurs around the zero-field temperature independent of the applied electric field strength. Slow cooling overcomes this barrier, and the disorder−order transition is observed only as the equivalent T_{ODT}^{h} for heating is reached. Therefore, we have access to a temperature regime $(T_{ODT}^{c}(0) > T > T_{ODT}^{h}(E))$, where reversible transitions between the ordered and disordered states can be achieved by application of a sufficiently high electric field strength E. This effect could be used to tailor samples by locally melting specific spots with spatially confined electric fields.

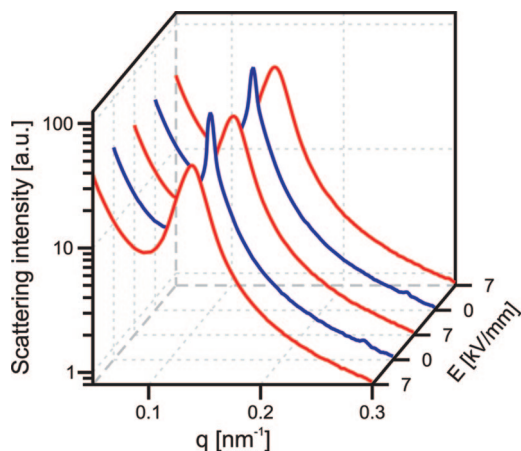**Figure 4.** SAXS spectra of a 32.5 wt % solution of SI in toluene at a constant temperature of $T = 53.0$ °C. The electric-field strength was switched between 7 kV/mm (disordered, red line) and 0 kV/mm (microphase separated, blue line).

Supporting Information Available: Comparison between a classical method using peak intensities to determine the T_{ODT} and our P_2-based method. This material is available free of charge via the Internet at http://pubs.acs.org.

References and Notes

(1) Debye, P.; Kleboth, K. *J. Chem. Phys.* **1965**, *42*, 3155.
(2) Wirtz, D.; Fuller, G. G. *Phys. Rev. Lett.* **1993**, *71*, 2236.
(3) Amundson, K.; Helfand, E.; Quan, X.; Hudson, S. D.; Smith, S. D. *Macromolecules* **1994**, *27*, 6559.
(4) Lin, C.-Y.; Schick, M.; Andelman, D. *Macromolecules* **2005**, *38*, 5766.
(5) Gunkel, I.; Stepanow, S.; Trimper, S.; Thurn-Albrecht, T. *Macromolecules* **2007**, *40*, 2186.
(6) Reich, S.; Gordon, J. M. *J. Polym. Sci., Part B: Polym. Phys.* **1979**, *17*, 371.
(7) Gurovich, E. *Macromolecules* **1994**, *27*, 7339.
(8) Onuki, A. *Europhys. Lett.* **1995**, *29*, 611.
(9) Orzechowski, K. *Chem. Phys.* **1999**, *240*, 275.
(10) Tsori, Y. *Nature (London)* **2004**, *430*, 544.
(11) Matsen, M. W.; Bates, F. S. *Macromolecules* **1996**, *29*, 1091.
(12) Xu, T.; Wang, J.; Russel, T. P. In *Nanostructured Soft Matter: Experiment, Theory, Simulation and Perspectives*, 1st ed.; Springer: Dordrecht, The Netherlands, 2007; p 171.
(13) Thurn-Albrecht, T.; Schotter, J.; Kastle, C. A.; Emley, N.; Shibauchi, T.; Krusin-Elbaum, L.; Guarini, K.; Black, C. T.; Tuominen, M. T.; Russell, T. P. *Science* **2000**, *290*, 2126.
(14) Schmidt, K.; Böker, A.; Zettl, H.; Schubert, F.; Hänsel, H.; Fischer, F.; Weiss, T. M.; Abetz, V.; Zvelindovsky, A. V.; Sevink, G. J. A.; Krausch, G. *Langmuir* **2005**, *21*11974.
(15) Schmidt, K.; Schoberth, H. G.; Schubert, F.; Hänsel, H.; Fischer, F.; Weiss, T. M.; Sevink, G. J. A.; Zvelindovsky, A. V.; Böker, A.; Krausch, G. *Soft Matter* **2007**, *3*, 448.
(16) Schmidt, K.; Schoberth, H. G.; Ruppel, M.; Zettl, H.; Hänsel, H.; Weiss, T. M.; Urban, V.; Krausch, G.; Böker, A. *Nat. Mater.* **2008**, *3*, 142.
(17) Böker, A.; Elbs, H.; Hänsel, H.; Knoll, A.; Ludwigs, S.; Zettl, H.; Zvelindovsky, A. V.; Sevink, G. J. A.; Urban, V.; Abetz, V.; Müller, A. H. E.; Krausch, G. *Macromolecules* **2003**, *36*, 8078.
(18) Sakamoto, N.; Hashimoto, T. *Macromolecules* **1995**, *28*, 6825.
(19) Amundson, K.; Helfand, E.; Davis, D. D.; Quan, X.; Patel, S. S.; Smith, S. D. *Macromolecules* **1991**, *24*, 6546.

MA900166W